

Holocene accumulation and ice sheet dynamics in central West Antarctica

T. A. Neumann, ^{1,2} H. Conway, ² S. F. Price, ^{2,3} E. D. Waddington, ² G. A. Catania, ^{2,4} and D. L. Morse ⁴

Received 1 February 2007; revised 17 August 2007; accepted 27 December 2007; published 23 May 2008.

[1] We derive depth-age relationships across the ice divide between the Ross and Amundsen Seas by tracking radar-detected layers from the Byrd ice core and a dated 105-m core near the divide. The depth-age relationships and an ice-flow model are used to establish histories of accumulation and ice sheet dynamics over the past 8000 years. Results show that accumulation was approximately 30% higher than today from 5000 to 3000 years ago. Antarctic climate variability today is dominated by periodic fluctuations in strength of the circumpolar vortex, which raises the possibility that the vortex was systematically weaker during the period of high accumulation. Accumulation today decreases almost linearly across the divide. It is unlikely that this pattern has changed through the Holocene. The radar-detected stratigraphy shows no evidence of the arched layers that are expected beneath a stable divide that is frozen to its bed, implying that the divide has also been migrating and/or the basal ice has been sliding through the Holocene. We cannot rule out the possibility of sliding because the basal ice is near its pressure melting point. Other evidence indicates that divide migration is likely. The Ross Sea sector is now near steady state, but it had a strong negative imbalance 200 years ago when Kamb Ice Stream was active. In contrast, recent speedups of Pine Island and Thwaites Glaciers have likely caused the mass balance of the Amundsen Sea sector to become negative. The divide is likely migrating toward the Ross Sea today.

Citation: Neumann, T. A., H. Conway, S. F. Price, E. D. Waddington, G. A. Catania, and D. L. Morse (2008), Holocene accumulation and ice sheet dynamics in central West Antarctica, *J. Geophys. Res.*, 113, F02018, doi:10.1029/2007JF000764.

1. Introduction

[2] Improved understanding of past climate and ice-thickness in central West Antarctica is needed to establish how the ice sheet will respond to current and future environmental change. Information about past accumulation and ice dynamics can be extracted from depth-age relationships measured today. Downward ice-flow velocity decreases with depth, and the associated strain rate pattern causes vertical thinning and horizontal stretching of layers. The thickness of an annual layer at depth in an ice sheet depends on both its initial thickness and the cumulative vertical strain since it was deposited. That is, an annual layer of ice-equivalent thickness b(t) when deposited at time t in the past at the surface, now has thickness $\lambda(t) = \Lambda(t)b(t)$. The thinning function $\Lambda(t) = 1 + \varepsilon(t)$, where $\varepsilon(t)$ is the cumulative vertical strain within the layer (excluding firm

[3] Depth-age relationships measured from ice cores can be extrapolated spatially by tracking continuous, radardetected internal layers [Dahl-Jensen et al., 1997; Arcone et al., 2004; Spikes et al., 2004]. We have tracked continuous radar-detected layers from the dated ice core at Byrd [Gow et al., 1968] and from a dated 105-m core [Dixon et al., 2004] to the ice divide between the Ross and Amundsen Seas (the Western Divide; see Figure 1). Here, we use the radar-derived depth-age relationships and a time-dependent, thermomechanical ice-flow model to determine histories of accumulation over the past 8000 years at three representative locations: the present-day divide; a site on the NE flank; and a site on the SW flank (Figure 1). The two flank sites (NE and SW) lie on flow lines that share a common point at the flow divide.

Copyright 2008 by the American Geophysical Union. 0148-0227/08/2007JF000764\$09.00

2. Data Sources and Methods

2.1. Byrd Timescale

[4] The Byrd ice core was drilled to bedrock in 1968 AD [Gow et al., 1968]. Damaged and missing core precluded counting of annual layers in the upper 88 m. Instead, a chronology was established by identifying the 1259 AD

F02018 1 of 9

compaction and densification) over time *t*. It follows that the layer-thickness profile (the derivative of the depth-age relationship) depends on both the history of accumulation and the history of ice dynamics.

¹Department of Geology, University of Vermont, Burlington, Vermont, USA.

²Department of Earth and Space Sciences, University of Washington, Seattle, Washington, USA.

³Fluid Dynamics Group, Los Alamos National Laboratory, Los Alamos, New Mexico, USA.

⁴Institute for Geophysics, Jackson School of Geosciences, University of Texas at Austin, Austin, Texas, USA.

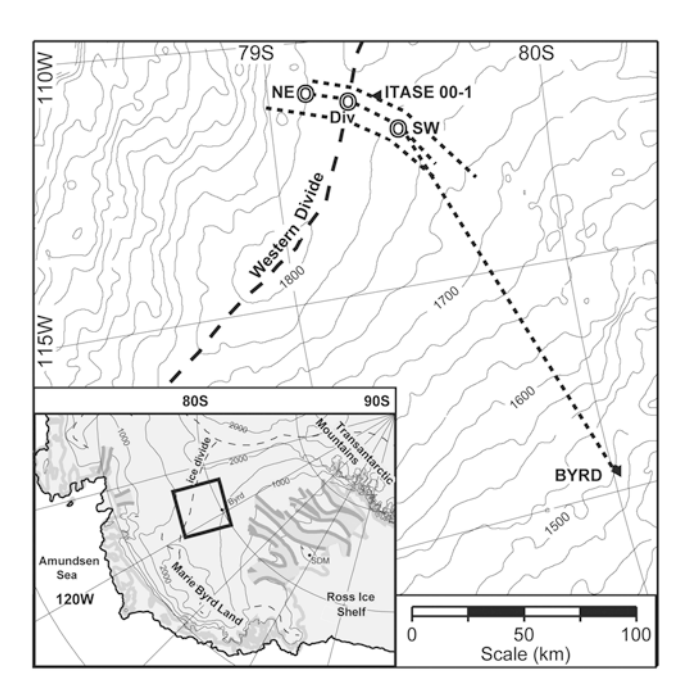


Figure 1. Surface elevations in the vicinity of the Western Divide, the ice divide between the Ross and Amundsen Seas, central West Antarctica (adapted from *Morse et al.* [2002]). Radar layers were tracked from a dated ice core at Byrd (80.017S, 119.517W) to the divide region. Primary radar lines are indicated by dashed lines; cross-profile transects are not shown. Sites NE, Div, and SW mark locations where accumulation histories are calculated. The two flank sites (NE and SW) lie on flow lines that share a common point at the flow divide (Div). A 105-m core was drilled at site ITASE 00-1 (79.383S, 111.229W) in 2000 AD. Drilling of a deep ice core (WAIS Divide ice core) started in 2006 AD near the SW site (79.468S, 112.086W).

volcanic horizon 97.8 m below the 1968 AD surface; mean annual accumulation over this 709-year period was 0.112 m a⁻¹ ice equivalent [Langway et al., 1988]. A timescale for the remainder of the core was established using the electrical conductivity method (ECM) [Hammer et al., 1994]. ECM-derived layer-thickness measurements were sparse in the brittle-ice zone (300–880 m below the surface) and so the measurements were fitted with three piecewise linear functions [Hammer et al., 1994]. The depth-age relationship was obtained by integrating the layer-thickness profile from the surface to depth. Blunier and Brook [2001] subsequently adjusted the timescale for the older (>12,000 yrs BP) sections of the core by correlating measurements of methane concentration at Byrd with those in layer-counted chronologies from Greenland.

2.2. ITASE 00-1 Timescale

[5] A 105-m core (ITASE 00-1) was extracted near the divide (Figure 1) in 2000 AD by the U.S. International Trans-Antarctic Scientific Expedition. The core contains well-preserved, seasonal chemistry back to 1651 AD; the layer-counted timescale and the density profile give an average accumulation over the 349-year interval of 0.25 m a⁻¹ ice equivalent [Dixon et al., 2004].

2.3. Radar Data

[6] We collected radar data during ground-based traverses in central West Antarctica during the 2002-03 and 2003-04 field seasons. Our system records a time domain voltage pulse induced in the receiving antennae. The center frequency of the voltage pulse depends on the antennae lengths; we used frequencies between 1 and 7 MHz. At these frequencies radar reflections are caused primarily by electrical conductivity contrasts inherited during snow deposition [Fujita et al., 1999], so that radar-detected layers can be treated as isochrones (layers of equal age). Two-way traveltime is converted to depth by assuming a wave speed of 168.5 m μs^{-1} in ice and 300 m μs^{-1} in air. Wave speed through the firn is calculated using the depth-density relationship measured in the ITASE 00-1 core and Looyenga's mixing equation [Glen and Paren, 1975] to estimate the dielectric constant of the ice/air mixture. The resolution (\sim 1/4 wavelength) is approximately \pm 6 m when using 7 MHz, and ±45 m when using 1 MHz. Uncertainty in the depth of a layer comes primarily from uncertainty in the wave speed in ice (about ± 2 m μ s⁻¹ which corresponds to about 1.2% of the depth to the layer) and also from picking the traveltime to the layer ($\pm 0.01 \mu s$, which corresponds to about ± 2 m).

[7] In central West Antarctica, we used 7 MHz antennae to detect layers from 30 m to about 1000 m below the surface. Measurements at 1 MHz were used to detect the bed, and layers deeper than 300 m below the surface. Figure 2a shows a 1-MHz profile between Byrd and the SW site (Figure 1). The oldest, continuous traceable layer ("old faithful") corresponds to multiple strong acid-depositional events between 1279.5 and 1283.5m in the Byrd core [Hammer et al., 1997], with corresponding age of \sim 17,400 yrs BP [Blunier and Brook, 2001]. Figure 2b shows a 1-MHz profile that follows a flow line up and over the divide (from the SW site to the NE site: see Figure 1). Ice thickness at the divide is 3280 m, where "old faithful" is 2460 m below the surface; the ice thickness is 3465 m at the SW site and 3350 m at the NE site. At an ice divide that is frozen to the bed, vertical velocity at mid-depths is lower than on the flanks, which causes radar-detected layers beneath a divide to be arched upward [Raymond, 1983]. Our radar-detected stratigraphy does not show such a distinctive stack of layering (known as a "Raymond" Bump") beneath the Western Divide (Figure 2b).

[8] We are unable to trace layers between 8400 and 17,400 yrs BP continuously from Byrd to the divide, which precludes resolving the details of accumulation and ice dynamics during that period. Here we focus attention on unraveling conditions over the past 8400 years. Figure 3a shows the Byrd timescale and the radar-derived timescale at the Western Divide for the past 8400 years. The layer-thickness profile (the derivative of the depth-age relationship) at the divide is shown in Figure 3b.

[9] Using isochronous layers in 7-MHz radar data, we spatially extrapolate the depth-age relationship measured at ITASE 00-1. Figure 4a shows a 7-MHz profile up and over the divide along the same line shown in Figure 2b. Figure 4b shows the spatial pattern of accumulation derived from seven individual radar-detected layers dated from the ITASE 00-1 core. The average ice-equivalent accumulation rate (averaged over the 349 years between 2000 and 1651 AD)

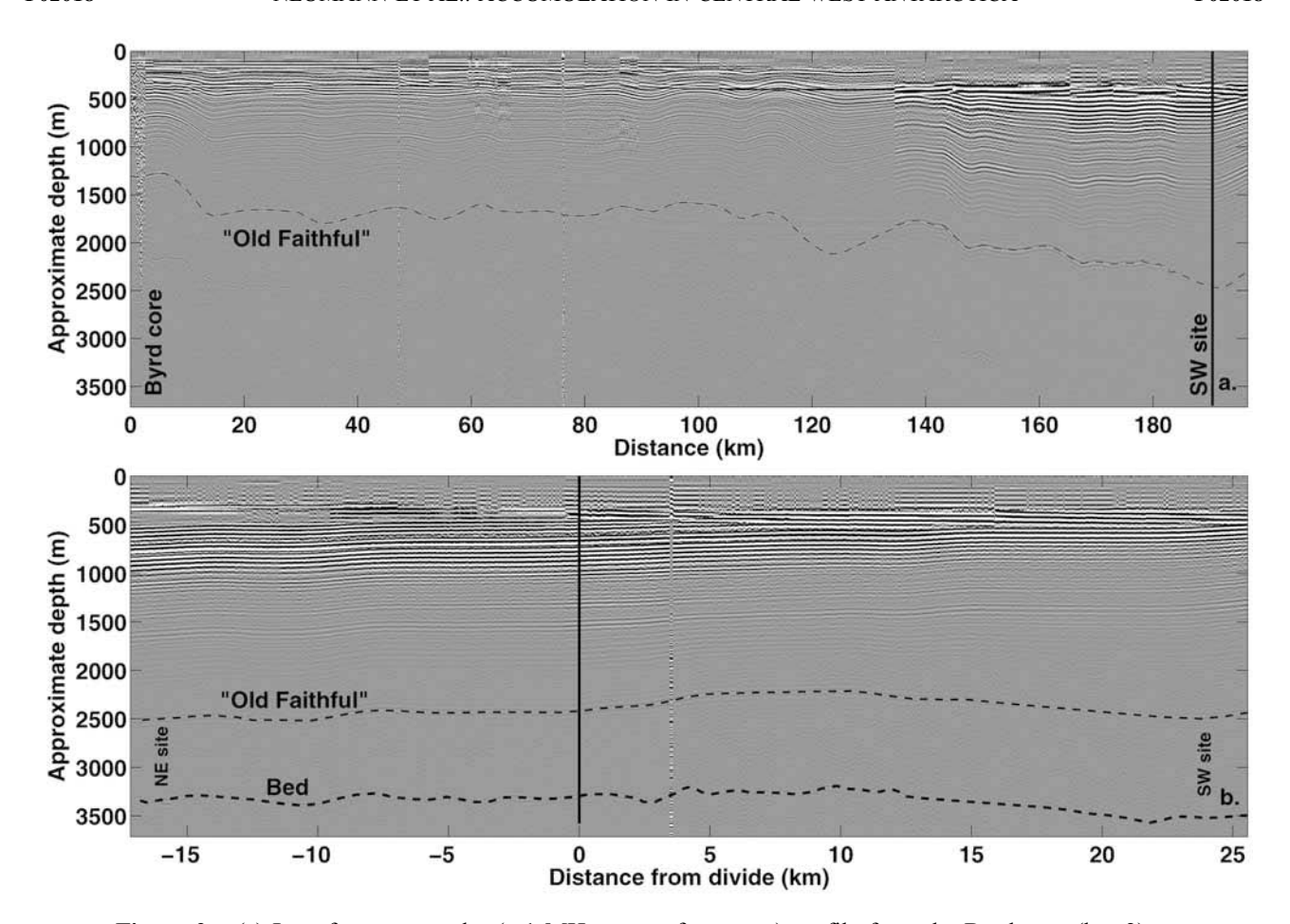


Figure 2. (a) Low-frequency radar (\sim 1 MHz center frequency) profile from the Byrd core (km 2) to near the SW site (km 193). Change in contrast at 135 km is due to a frequency change from 1.5 to 1 MHz. The deepest continuous layer (\sim 1300 m at Byrd) corresponds to a strong acid-deposition event that is dated at 17,400 years BP at Byrd [*Hammer et al.*, 1994]. (b) Low-frequency radar (\sim 1 MHz center frequency) profile from the SW site across divide (Div) to the NE site. Ice thickness along the profile varies from 3450 m at the SW site, 3280 m at the divide, to 3350 m at the NE site. Notably lacking in the stratigraphy is a distinctive stack of arched layers that is expected beneath a divide that is stable and frozen to its bed [*Raymond*, 1983].

varies from $0.22~\text{m a}^{-1}$ at the SW site, $0.27~\text{m a}^{-1}$ at the divide, to $0.34~\text{m a}^{-1}$ at the NE site. Relative to the divide, the modern accumulation is approximately 25% higher 16 km northeast of the divide, and 20% lower 24 km southwest of the divide.

3. Models

3.1. Transient Ice-Flow Model

[10] We use a kinematic ice-flow model with simplified ice dynamics. A more sophisticated model is not warranted because detailed information about spatial and temporal variations of ice rheology, effective stress and temperature is not available. In the model, the horizontal and vertical velocity equations are coupled through shape functions that satisfy mass continuity [Reeh, 1988]. Following Dansgaard and Johnsen [1969], we approximate the horizontal velocity with two piecewise linear functions in which velocity is uniform with depth in the upper part of the ice sheet, and then decreases linearly to zero at the bed below height h (measured from the bed). With these assumptions, the

time-dependent vertical velocity field w(z, t) can be written

$$w(z,t) = -\frac{\dot{a}(t)[z - h(t)/2]}{[H(t) - h(t)/2]} + \dot{m}(t) \qquad H(t) \ge z \ge h(t)$$

$$w(z,t) = -\frac{\dot{a}(t)z^2}{2h(t)[H(t) - h(t)/2]} + \dot{m}(t) \qquad h(t) \ge z \ge 0$$
(1)

where the "flux-effective" mass balance $\dot{a}(t) = \dot{b}(t) + \dot{m}(t) - \dot{H}(t)$ includes terms for surface accumulation $\dot{b}(t)$, basal melting $\dot{m}(t)$ (negative for melting), and changes of ice thickness $\dot{H}(t)$ (negative for thinning).

[11] Our choice of values for model parameter h(t) is guided by previous studies and results from the Western Divide using a full-stress flow-model. Siple Dome in West Antarctica is frozen at the bed, and *Nereson et al.* [1998a] showed that using $h_{\text{flank}} = 0.2 \, H$ on the flanks (more than $1.0 \, H$ distant from the divide) and $h_{\text{div}} = 0.7 \, H$ at the divide yields a good approximation to the vertical-velocity shape

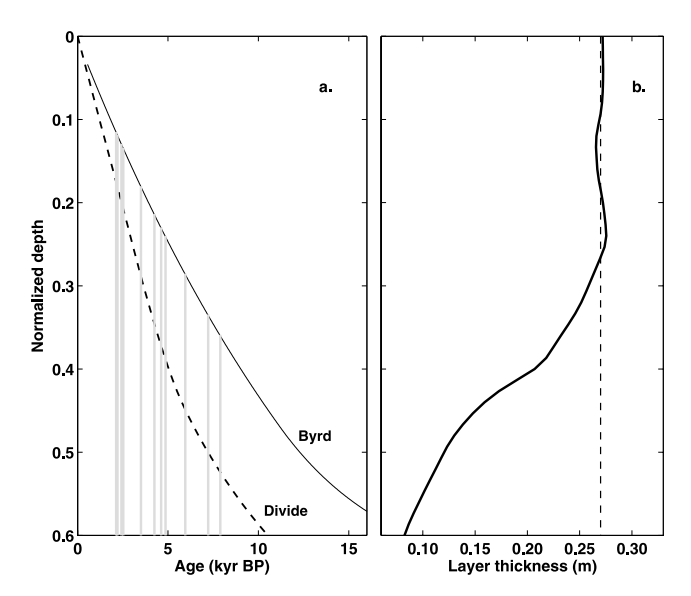


Figure 3. (a) Depth-age relationships at Byrd [from *Hammer et al.*, 1994], and at the divide derived from continuous isochronous radar-detected layers tracked from Byrd; vertical gray lines show tie points. Depths are normalized by total ice-equivalent thickness at each site (2164 m at Byrd, and 3280 m at the divide). (b) Layer-thickness profile (the derivative of the depth-age relationship) at the divide.

functions predicted by a full-stress, thermomechanical model. Grinsted and Dahl-Jensen [2002] used a Monte-Carlo tuned flow model and found values ranging from 0.63~H to 0.97~H with an average value h = 0.77~H at NorthGRIP, a divide site that is melting at the bed in Greenland. At the Western Divide we use a two-dimensional, full-stress, thermomechanical model [Price et al., 2007] to calculate the steady state velocity field under present-day conditions. Results show that if the divide is frozen to the bed, the vertical velocity profile is well approximated by using $h_{\text{flank}} = 0.2 \text{ H}$ on the flanks and $h_{\text{div}} = 0.7 \text{ H}$ at the divide. However, if the divide has been moving around over distances >1.0 H (>3.5 km) at speeds faster than \sim 3 \times b $(\sim 1 \text{ m a}^{-1})$, the time-averaged vertical velocity profile at the present-day divide will be some mix of divide-like and flank-like flow [Nereson and Waddington, 2002]; that is, for a migrating divide 0.2 $H < h_{\text{div}} < 0.7 H$. In addition, *Pettit et* al. [2003] showed that even a small amount of basal sliding beneath a divide could cause the vertical velocity profile to be more similar to that on the flanks.

[12] Following the approach of *Waddington et al.* [2005], we use a simplified ice-flow model (equation (1)) to calculate depth-age relationships for various combinations of histories of accumulation, basal melting and ice dynamics. By ice dynamics, we mean the history of ice thickness H(t) and the history of vertical strain rate, which is determined by H(t) and h(t). We accept combinations that produce modeled depth-age relationships that match the radar-detected depth-age relationships to within the data uncertainty. We start by prescribing constant H(t), h(t) and m(t) through time, and we adjust b(t) to produce modeled depth-age relationships that match the radar-derived depth-

age relationship. We then explore the sensitivities to a transient ice-thickness history, and to different combinations of [h(t)/H(t)] and $\dot{m}(t)$.

3.2. Transient Thermal Model

[13] The temperature profile in an ice sheet depends on histories of surface temperature, accumulation rate, vertical velocity, and geothermal flux. Near an ice divide, horizontal advection of heat is small, and we use a one-dimensional, finite-volume [Patankar, 1980], advection-diffusion model to calculate temperature profiles through the ice column and 15 km below the ice-bed interface. Vertical velocity of the ice is calculated from equation (1), and we account for temperature- and density-dependent thermal properties of the ice column [Paterson, 1994, p. 205], and pressuredependent melting [Hobbs, 1974]. We use the density profile from the ITASE 00-1 core to estimate thermal properties in the firn. We calculate an initial steady state temperature profile 250,000 yrs BP using the formulation of Firestone et al. [1990], after which the temperature profile evolves in 200-year time steps. By placing the lower boundary condition effectively at infinity, our results are not sensitive to the boundary condition applied at the base of the bedrock; the 250,000 year model run allows the upper part of the bedrock to adjust to the most recent 100,000 year cycle. Present-day ice thickness comes from radar sounding (Figure 2b). The 10-m temperature was not measured at ITASE 00-1 and so the mean annual temperature at the divide (-31°C) is estimated by applying a lapse rate of -10° C km⁻¹ to the measured value at Byrd. This value is consistent with recent measurements based on atmospheric data at the WAIS Divide drilling site.

[14] We assume that the ice-thickness and surface temperature during the last interglacial (120,000 yrs BP) were similar to today and we run the model forward in time using the histories shown in Figure 5. At each site, we use the accumulation-rate history that we infer from the internal layers, using our ice-flow model. Prior to 8400 years B.P. we use the modern accumulation rate at each site. Since the accumulation-rate and ice-thickness histories are not coupled in our model, the depth to layers deposited since 8400 years B.P. are not influenced by accumulation variations prior to deposition.

[15] In the model, basal-melt rate responds instantaneously to changes in ice thickness through the pressure-melting term. Although changes in accumulation affect the vertical velocity field, the temperature profile and the basal melt rate have a lagged response to accumulation changes due to the finite time required for the vertical advection of warmer (or colder) ice. Surface-temperature perturbations also have a lagged effect on the temperature profile and the basal melt rate. In the vicinity of the divide, for a given geothermal flux, the basal-melt rate is controlled primarily by the histories of ice thickness and accumulation rate; details of the surface-temperature history are of secondary importance.

4. Results

4.1. Accumulation and Ice Dynamics at the Divide

[16] Accumulation at the divide averaged over the 349 years since 1651 AD (0.27 m $\rm a^{-1}$) is approximately 13% lower than the value of 0.31 m $\rm a^{-1}$ calculated by *Morse et al.*

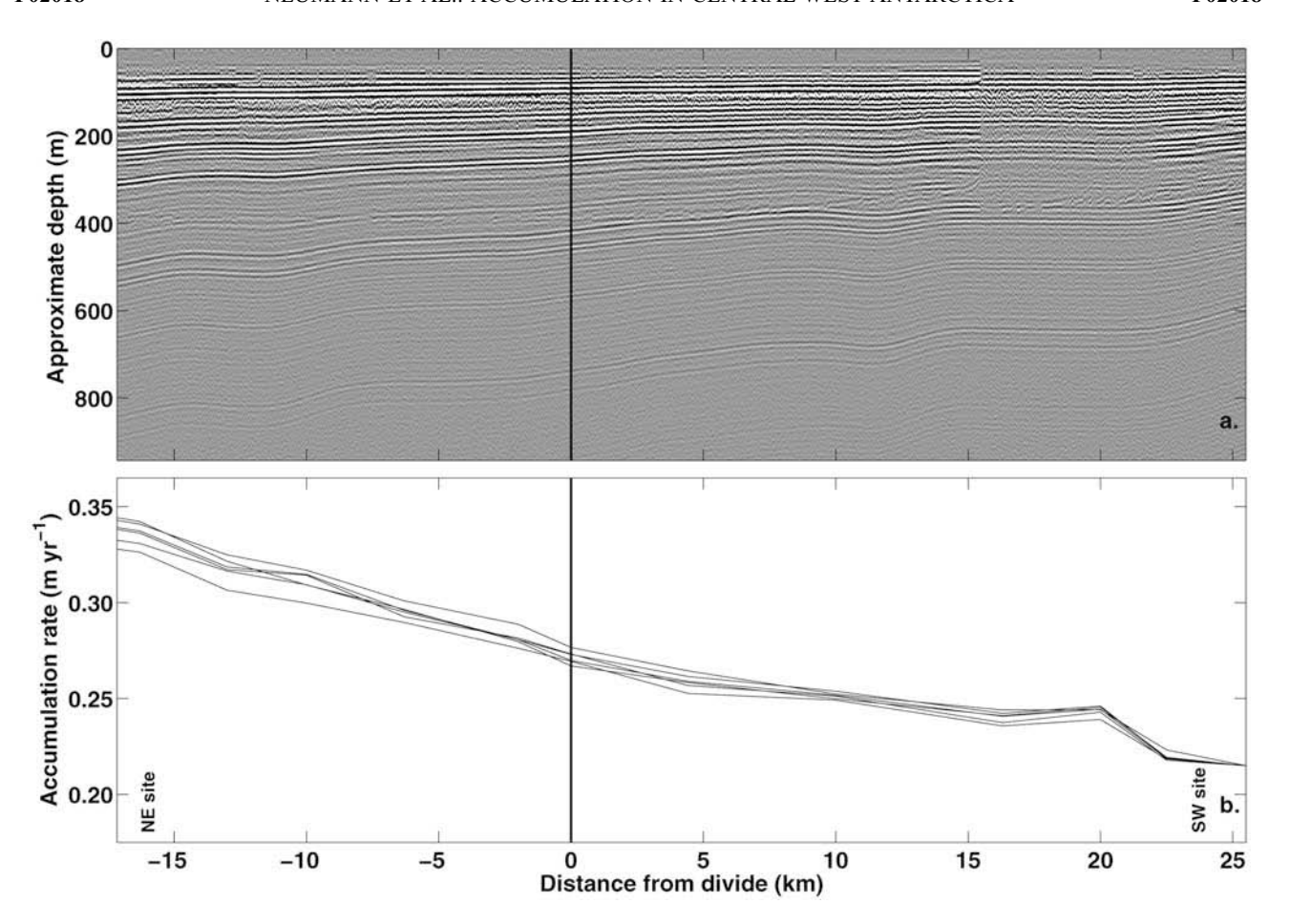


Figure 4. (a) Radar-profile (\sim 7 MHz center frequency) from the SW site, across the divide, to the NE site. Age control for the radar-detected layers is provided by the depth-age relationship from ITASE 00-1, and the layers extrapolate the age field. (b) Spatial pattern of ice-equivalent accumulation derived from seven individual radar-detected layers dated from the ITASE 00-1 core. The average ice-equivalent accumulation rate (averaged over the 349 years between 2000 and 1651 AD) increases from 0.22 m a⁻¹ at the SW site, to 0.27 m a⁻¹ at the divide, to 0.34 m a⁻¹ at the NE site.

[2002] as an average over the past 2500 years, giving the first indication that accumulation has decreased over the past 2500 years.

[17] The second indication that accumulation at the divide has been decreasing comes from the radar-derived layer-thickness profile. The thicknesses of annual layers up to 2500 years old are nearly uniform (Figure 3b) and the simplest explanation for this unusual pattern is that $\dot{b}(t)$ has been decreasing for the past 2500 years.

[18] It is possible that reduced extensional horizontal strain rate (i.e., reduced stretching) over the past 2500 years also contributed to the pattern by preventing individual layers from thinning over time, but reduced stretching alone cannot produce the observed profile; absence of longitudinal strain, or even compressive longitudinal strain, necessary for a layer to thicken over time, is not physically reasonable at a flow divide that is located near the center of an ice sheet. In addition, absence of longitudinal strain over the past 2500 years would have allowed ongoing accumulation to thicken the ice sheet by over 600 m during that interval, because there would have been no horizontal flow to evacuate ice from the divide region. Such thickening is highly implausible, given that other areas on the ice sheet

show little or no change [e.g., Steig et al., 2001; Waddington et al., 2005].

[19] We use the model (equation (1)) to quantify the history of accumulation. Most reconstructions of West Antarctica call for an ice sheet that was thicker than today during the last glacial maximum, requiring overall thinning through the Holocene. *Steig et al.* [2001] compared stable-isotope profiles in the Byrd and Taylor Dome ice cores to derive a history that includes 300 m of thinning followed by 100 m thickening at Byrd during the Holocene (Figure 5a). Although we expect thickness changes at the divide to have been less than those at Byrd on the flank of the ice sheet, we compare model results for this end-member history against those calculated with no thickness change (Figure 6a).

[20] Other things being equal, more accumulation is needed to produce the same depth-age relationship in an ice sheet that has thinned compared with an ice sheet of constant thickness. However, in the thick ice near the divide, a thickness change of 200 m over the past 9,000 years has negligible impact on the inferred accumulation history (Figure 6a); fractional thinning (200 m/3280 m) over 9,000 years would induce strain rates of $\sim 10^{-5}$ a⁻¹, which are an order of magnitude less than strain rates expected in

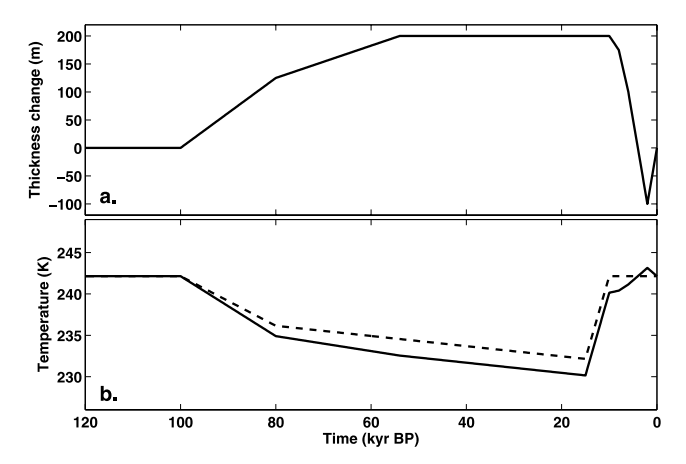


Figure 5. Assumed histories of ice-thickness change (a) and surface temperature (b) for the past 120,000 years at the divide. Present ice thickness at the divide is 3280 m ice equivalent. Panel (a) shows ice-thickness history through the Holocene, taken from *Steig et al.* [2001]. Panel (b) shows the climate-temperature history (dashed curve) and the surface-temperature history (solid curve), which is adjusted for prescribed elevation (ice thickness) changes in (a). Present-day surface temperature at the divide (-31°C) is estimated by applying a lapse rate of $-10^{\circ}\text{C km}^{-1}$ to the measured value at Byrd.

the upper section of the ice sheet for the case of no thinning. Hence our inferred accumulation history is relatively insensitive to the modest changes in thickness expected near the ice divide during the Holocene. Although this means that we cannot resolve the details of ice-thickness changes through the Holocene, we do have confidence in our inferred accumulation history because it is not confounded by uncertainty in H(t).

[21] Annual layers that have been deposited relatively recently have not yet accumulated sufficient total strain to be able to determine the present-day value of h_{div} , and so our inferred accumulation history is insensitive to the present value of h_{div} . Given that the ice dynamics beneath the present divide may have changed during deglaciation because of divide migration and/or a switch from frozen to thawed basal conditions, we use the model to estimate b(t)with the two end-member cases for the dynamics at the divide: (1) $h_{\text{div}} = 0.7 H$ to represent a stable divide frozen to its bed; (2) $h_{\text{div}} = 0.2 \text{ H}$ to represent a divide with basal sliding, or one that has been continually migrating over the past 8000 years. Results show that for both cases, relatively high accumulation between 5000 and 3000 yrs BP (Figure 6a) is necessary to match the depth-age relationship (Figure 3a); maximum Holocene accumulation varies from 30% to 70% greater than present, depending on the value of h_{div} chosen to represent the strain rate field.

4.2. Accumulation and Ice Dynamics on the Flanks

[22] We also derive accumulation histories for a flank site 16 km north and east of the present divide location, and another 24 km to the south and west (Figure 1). We assume that both sites have always been on the flank of the ice sheet, and $h_{\rm flank} = 0.2 \, H$. One-dimensional ice-flow assumptions are not valid for sites so far from a divide, especially in

regions where gradients in accumulation and ice thickness exist. We use a two-dimensional model [Price et al., 2007] to track particle paths back to the surface from the flank sites. Results indicate that ice in the oldest layer used in this analysis (8400 yrs BP) at the SW site originated at 13 km upstream, where accumulation today is 12% higher (Figure 4b). Advection of ice from upstream has less consequence for younger layers because progressively younger layers originated at locations progressively closer to the flank sites of interest. We calculate $\dot{b}(t)$ for the site (Figure 6b) by assuming that the modern accumulation gradient has persisted through time. Similar calculations indicate that ice in the 8400-year old layer at the NE site would have originated from a location approximately 12 km upstream, where accumulation today is 17% lower (Figure 4b).

4.3. Basal Melting

[23] The geothermal flux in West Antarctica is not well constrained, but estimates derived from borehole temperature profiles range from 69 mW m⁻² at Siple Dome [*Engelhardt*, 2004] to 75 mW m⁻² at Byrd [*Gow et al.*, 1968]. At the SW

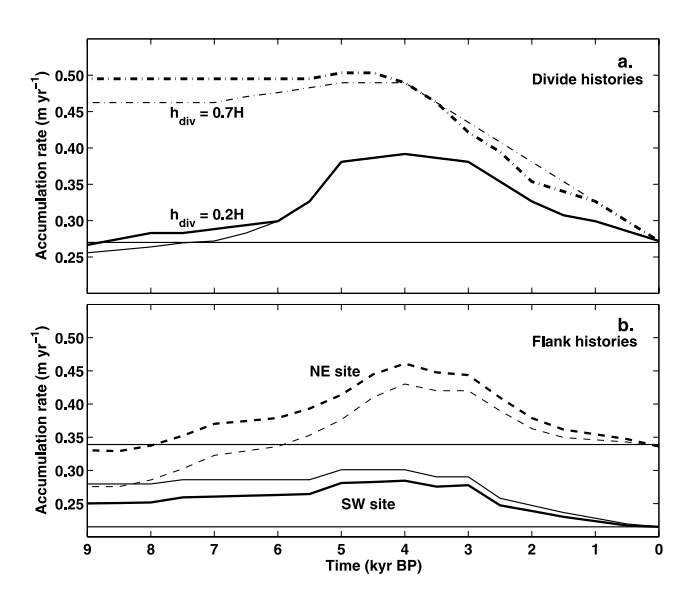


Figure 6. (a) Inferred accumulation history at the divide using $h_{\rm div} = 0.7 \ H$ (dashed curves), appropriate for a stable divide that is frozen to its bed, and $h_{\text{div}} = 0.2 \text{ H}$ (solid curves) appropriate if the basal ice has been sliding and/or the divide has been migrating over time. Compared with cases of no thinning (thin line in each case), slightly more accumulation (thick line in each case) is necessary to compensate for the thickness history shown in Figure 5a. Thin horizontal line indicates today's accumulation rate. (b) Modeled accumulation histories for the two flank sites, assuming $h_{\text{flank}} = 0.2 \text{ H}$ and using the thinning history shown in Figure 5a. Ice at depth at the NE site originated nearer the divide where accumulation is lower; accumulation at the NE site (thick dashed line) has been higher than that calculated without allowing for advection (thin dashed line). Similarly, ice at depth at the SW site originated in a region of higher accumulation; accumulation at the SW site (thick solid line) has been lower than that calculated without allowing for advection (thin solid line).

site (assuming $h_{\text{flank}} = 0.2 \text{ H}$) the model predicts basal melting at all times if the geothermal flux exceeds 70 mW m^{-2} . At the divide, if $h_{div} = 0.7$ H, melting is likely at all times if the geothermal flux exceeds 65 mW m⁻². However, if $h_{\text{div}} = 0.2 \, H$, cold surface ice is advected downward faster and a geothermal flux in excess of 100 mW m⁻² is needed to cause basal melting at all times. At the NE site (assuming $h_{\text{flank}} = 0.2 \text{ H}$) where accumulation is higher, the model predicts melting at all times only if the geothermal flux exceeds 100 mW m⁻². Model runs with lower geothermal flux show melting at all times except during the period of high accumulation rate (5000 to 3000 years BP); the combined effects of ice sheet thickening and decreasing accumulation over the past 2000 years cause basal melting to start again at the NE site around 1000 years BP. Note that for the thermal calculation, we prescribe accumulation prior to 8400 years BP to be the same as present. In reality, we expect that accumulation was less than the present value during the last glacial maximum, and so our inferred value for the geothermal flux required to initiate melting is likely an upper estimate. In summary, results from thermal modeling suggest that the bed is currently wet at the SW site, and that there is a transition from frozen to thawed basal conditions within a few ice thicknesses of the present divide.

5. Discussion

5.1. History of Accumulation

[24] Relatively high accumulation from 5000 to 3000 yrs BP emerges as a robust feature at all three sites (Figure 6); we conclude that accumulation was more than 30% higher than present during that time. This is consistent with findings of *Siegert and Payne* [2004] who also inferred relatively high accumulation 100 km farther north and east during the mid-Holocene.

[25] Ice core measurements [e.g., Dixon et al., 2004; Kreutz et al., 2000] and atmospheric models of moisture and sublimation fluxes [Bromwich et al., 2000; Noone and Simmonds, 2002; van den Broeke and van Lipzig, 2004] indicate that inter-annual variations of accumulation in West Antarctica today often exceed 30%. Climate variability in the high-latitude Southern Hemisphere is dominated by the Antarctic Oscillation (AAO) [Thompson and Wallace, 2000], which represents fluctuations in the strength of the circumpolar vortex. van den Broeke and van Lipzig [2004] used a regional climate model to show that when the circumpolar vortex is strong (high AAO index), precipitation decreases up to 30% in West Antarctica and increases by $\sim 30\%$ on the western side of the Antarctic Peninsula, and vice versa. On the basis of the present-day climatology, a possible explanation for high accumulation in West Antarctica during the mid-Holocene might be that the circumpolar vortex was biased toward a weak mode during that period. However, the relatively short observational record (at most up to 50 years) hampers our understanding of climate variability in Antarctica. Coupled ocean-climate models can help us to understand physical processes underlying climate change in Antarctica. Spatial and temporal climate-proxy data inferred from spatially distributed cores combined with ice stratigraphy from ice-penetrating radar can help to constrain and validate those climate models.

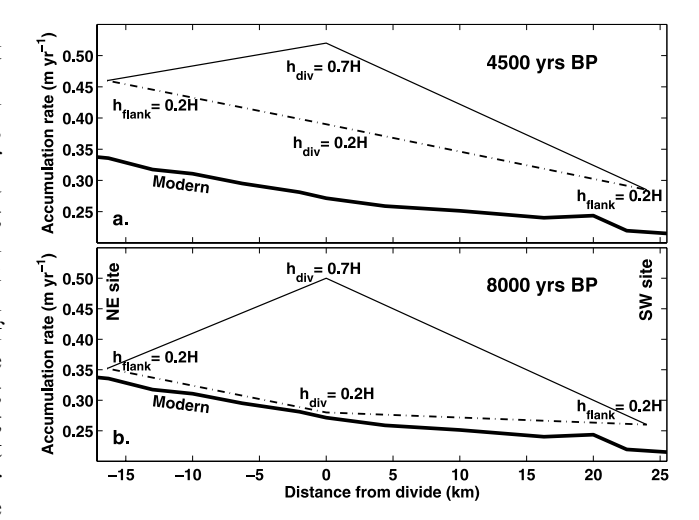


Figure 7. Modern spatial pattern of accumulation across the divide (thick-solid line) averaged over the 349-year interval prior to 2000 AD, compared with reconstructions of spatial patterns (a) at 4500 yrs BP, and (b) at 8000 yrs BP. All model reconstructions used thinning history shown in Figure 5a. Ice dynamics are represented by $h_{\rm flank} = 0.2~H$ for both flank sites, and $h_{\rm div} = 0.7~H$, appropriate for a stable divide that is frozen to its bed, or $h_{\rm div} = 0.2~H$, appropriate if the basal ice has been sliding and/or the divide has been moving around. Using $h_{\rm div} < 0.7~H$ generates a spatial pattern that is more consistent with today's near-uniform gradient.

The near-linear variation in present-day accumulation across the divide (Figure 4b) suggests that the orographic effect of the divide crest on accumulation is small. This pattern is consistent with results of *van den Broeke et al.* [2006] who point out that persistent onshore flow of moisture-bearing air masses in combination with steep coastal topography in the Amundsen Sea results in high accumulation (~0.8 m yr⁻¹) near the coast and progressively decreasing accumulation inland.

5.2. History of Divide Position

[26] The spatial pattern of accumulation provides insight into the likely ice-flow history in the vicinity of the divide. Model results show that accumulation histories calculated by parameterizing the vertical-velocity field with $h_{\rm div} > 0.2\,H$ require changes in the accumulation gradient through time; larger values of $h_{\rm div}$ require progressively more accumulation at the divide to match the radar-detected depth-age relationship (Figure 7). However, there is no reason to think that the divide had a strong orographic affect on accumulation in the past, and we conclude that a persistent spatial pattern with today's near-uniform accumulation gradient is more physically reasonable.

[27] Following this line of reasoning, our results indicate that using $h_{\rm div}=0.2~H$ provides a better match to the expected pattern of accumulation in the past, which suggests that on average, ice flow at the divide has been more similar to flank flow than divide flow. This finding indicates that either the location of the divide has not been stable through time [Nereson and Waddington, 2002] and/or the presence of basal sliding [Pettit et al., 2003]. This conclu-

sion is supported by the radar-detected internal stratigraphy across the divide (Figure 2b) which do not show the distinctive pattern of upwarped layering that occurs beneath a divide that is stable and frozen to its bed [Raymond, 1983].

[28] Nereson and Waddington [2002] showed that the shape of radar-detected layers beneath a divide contains a history of divide positions, but the lack of evidence for a "Raymond Bump" at the Western Divide (Figures 2b and 4a) prevents us from resolving the histories of divide migration and/or basal sliding. We cannot rule out the possibility of basal sliding because uncertainties in the geothermal flux and in the histories of accumulation and thinning preclude an accurate estimate of the basal-melt history at the divide (section 4.3). Small asymmetric changes at the boundaries of an ice sheet or in the accumulation gradient can cause an ice divide to migrate [Nereson et al., 1998b]. The relaxation time for divide position adjustment is a small fraction of the characteristic thickness/accumulation rate (H/b) timescale [Hindmarsh, 1996]; the relaxation time for the Western Divide is expected to be on the order of 600 years. Asymmetric changes at the boundaries of the Western Divide are a real possibility because observations indicate that the Ross Sea sector is now near steady state, but it likely had a strong negative imbalance 200 years ago when Kamb Ice Stream was still active [Joughin and Tulaczyk, 2002]. In contrast, observations from the Amundsen Sea sector show a recent speedup and thinning of Pine Island and Thwaites Glaciers [Joughin et al., 2003; Rignot, 2002; Shepherd et al., 2001, 2002]. Although there is some uncertainty, it is likely that the mass balance of the Amundsen Sea sector is now negative. Under these conditions we expect that the divide is migrating toward the Ross Sea today.

6. Conclusions

- [29] Depth-age relationships in an ice sheet contain a record of past accumulation and cumulative strain. First-order information about the histories of accumulation rate and ice sheet dynamics can be extracted using a simplified one-dimensional ice-flow model. Some caution is needed, however, when applying one-dimensional models to flank sites, because advection of ice deposited upstream may become important, especially at locations where gradients in accumulation and/or ice thickness are large.
- [30] Relatively high accumulation from 5000 to 3000 yrs BP across the Western Divide emerges as a robust result that is relatively insensitive to the modest thickness changes expected there during the Holocene. Our result depends on the fidelity of the timescale from the Byrd core. Verification will come from the high-resolution depth-age relationship from the new WAIS Divide ice core. Data from this core will allow us to infer histories of accumulation and ice sheet dynamics back through the last glacial maximum.
- [31] Model results and the radar-detected stratigraphy indicate that the ice divide has been moving, and/or the ice at the divide is sliding at the bed. We cannot rule out the possibility of sliding at the bed, but the present-day asynchronous thinning on either side of the divide suggests that peregrinations of the Western Divide have likely occurred throughout the Holocene.

- [32] Ice cores are often drilled near ice divides in order to minimize stratigraphic disturbance caused by horizontal shearing of ice [e.g., Waddington et al., 2001]. However, model results from Greenland [Marshall and Cuffey, 2000] suggest that changes in flow associated with migration of the Greenland summit may have contributed to the stratigraphic disruption of Eemian ice in the GRIP and GISP2 cores. The location of the new WAIS Divide core site (24 km from the present-day divide) was chosen as a compromise between being far enough away to minimize the possibility that the divide has migrated through that site, and yet close enough to minimize stratigraphic disturbances caused by horizontal shearing of the ice. Nevertheless, caution will be needed when interpreting stratigraphic sequences in the WAIS Divide core.
- [33] Acknowledgments. This work was supported by grants from the US National Science Foundation (OPP-0087345, OPP-0125610, and OPP-0440666). We also thank: P. A. Mayewski and D. A. Dixon, who provided unpublished data from the ITASE 00-1 core; M. Conway, K. Matsuoka, F. Ng and E. Pettit, who assisted in the field; Raytheon Polar Services, Air National Guard and Ken Borek Air for logistical support; and R. C. A. Hindmarsh, E. King, S. Marshall, T. Murray and B. Welch for constructive comments on earlier drafts of the manuscript.

References

- Arcone, S. A., V. B. Spikes, G. S. Hamilton, and P. A. Mayweski (2004), Stratigraphic continuity in 400-MHz short-pulse radar profiles of firn in West Antarctica, *Ann. Glaciol.*, *39*, 195–200.
- Blunier, T., and É. J. Brook (2001), Timing of millennial-scale climate change in Antarctica and Greenland during the last glacial period, *Science*, 291, 109–112.
- Bromwich, D. H., A. N. Rogers, P. Kållberg, R. I. Cullather, J. W. C. White, and K. J. Kreutz (2000), ECMWF analyses and reanalyses depiction of ENSO signal in Antarctic precipitation, *J. Clim.*, 13, 1406–1420.
- Dahl-Jensen, D., N. S. Gundestrup, K. R. Keller, S. J. Johnsen, S. P. Gogineni, C. T. Allen, T. S. Chuah, H. Miller, S. Kipstuhl, and E. D. Waddington (1997), A search in north Greenland for a new ice-core drill site, *J. Glaciol.*, 43(144), 300–306.
- Dansgaard, W., and S. J. Johnsen (1969), A flow model and a time-scale for the ice core from Camp Century, Greenland, *J. Glaciol.*, 8(53), 215–223. Dixon, D. A., P. A. Mayewski, S. Kaspari, S. Sneed, and M. Handley (2004), A 200-year sub-annual record of sulfate from 16 ice cores,
- Ann. Glaciol., 39, 545–556.
 Engelhardt, H. (2004), Ice temperature and high geothermal flux at Siple Dome, West Antarctica, from borehole measurements, *J. Glaciol.*, 50(169), 251–256.
- Firestone, J., E. D. Waddington, and J. Cunningham (1990), The potential for basal melting under Summit, Greenland, *J. Glaciol.*, 36(123), 163–168
- Fujita, S., H. Maeno, S. Uratsuka, T. Furukawa, S. Mae, Y. Fujii, and O. Watanabe (1999), Nature of radio echo layering in the Antarctic ice sheet detected by a two-frequency experiment, *J. Geophys. Res.*, 104, 13,013–13,024.
- Glen, J. W., and J. G. Paren (1975), The electrical properties of snow and ice, *J. Glaciol.*, 15(73), 15–38.
- Gow, A. J., H. T. Ueda, and D. E. Garfield (1968), Antarctic ice sheet: Preliminary results of first core hole to bedrock, *Science*, *161*, 1011–1013
- Grinsted, A., and D. Dahl-Jensen (2002), A Monte Carlo-tuned model of the flow in the NorthGRIP area, *Ann. Glaciol.*, *35*, 527–530.
- Hammer, C. U., H. B. Clausen, and C. C. Langway (1994), Electrical conductivity method (ECM) stratigraphic dating of the Byrd Station ice core, Antarctica, *Ann. Glaciol.*, 20, 115–120.
 Hammer, C. U., H. B. Clausen, and C. C. Langway (1997), 50,000 years of
- Hammer, C. U., H. B. Clausen, and C. C. Langway (1997), 50,000 years of recorded global volcanism, *Clim. Change*, 35, 1–15.
- Hindmarsh, R. C. A. (1996), Stochastic perturbation of divide position, Ann. Glaciol., 23, 94-104.
- Hobbs, P. V. (1974), *Ice Physics*, Oxford Univ. Press., London.
- Joughin, I., and S. Tulaczyk (2002), Positive mass balance of the Ross Ice Streams, West Antarctica, Science, 295, 476–480.
- Joughin, I., E. Rignot, C. E. Rosanova, B. K. Lucchitta, and J. Bohlander (2003), Timing of recent accelerations of Pine Island Glacier, Antarctica, *Geophys. Res. Lett.*, 30(13), 1706, doi:10.1029/2003GL017609.

- Kreutz, K. J., P. A. Mayewski, L. D. Meeker, M. S. Twickler, and S. I. Whitlow (2000), The effect of spatial and temporal accumulation rate variability in West Antarctica on soluble ion deposition, *Geophys. Res. Lett.*, 27, 1520–2517.
- Langway, C. C., H. B. Clausen, and C. U. Hammer (1988), An inter-hemispheric volcanic time-marker in ice cores from Greenland and Antarctica, Ann. Glaciol., 10, 102–108.
- Marshall, S. J., and K. M. Cuffey (2000), Peregrinations of the Greenland Ice Sheet divide in the last glacial cycle: Implications for central Greenland ice cores, *Earth Planet. Sci. Lett.*, 179, 73–90.
- Morse, D. L., D. D. Blankenship, E. D. Waddington, and T. A. Neumann (2002), A site for deep ice coring in West Antarctica: Results from aerogeophysical surveys and thermo-kinematic modeling, *Ann. Glaciol.*, 35, 36–44
- Nereson, N. A., and E. D. Waddington (2002), Isochrones and isotherms beneath migrating ice divides, *J. Glaciol.*, 48(160), 95–108.
- Nereson, N. A., C. F. Raymond, E. D. Waddington, and R. W. Jacobel (1998a), Migration of the Siple Dome ice divide, West Antarctica, *J. Glaciol.*, 44, 643–652.
- Nereson, N. A., R. C. A. Hindmarsh, and C. F. Raymond (1998b), Sensitivity of the divide position at Siple Dome, to boundary forcing, *Ann. Glaciol.*, 27, 207–214.
- Noone, D., and I. Simmonds (2002), Annular variations in moisture transport mechanisms and the abundance of δ^{18} O in Antarctic snow, *J. Geophys. Res.*, 107(D24), 4742, doi:10.1029/2002JD002262.
- Patankar, S. V. (1980), Numerical heat transfer and fluid flow, Hemisphere Publishing, New York.
- Paterson, W. S. B. (1994), Physics of Glaciers, third edition, Elsevier, Oxford.
- Pettit, E. C., H. P. Jacobson, and E. D. Waddington (2003), Effects of basal sliding on isochrones and flow near an ice divide, *Ann. Glaciol.*, *37*, 370–376.
- Price, S. F., E. D. Waddington, and H. Conway (2007), A full-stress thermomechanical flowband model using the finite-volume method, *J. Geophys. Res.*, 112, F03020, doi:10.1029/2006JF000724.
- Raymond, C. F. (1983), Deformation in the vicinity of ice divides, J. Glaciol., 29(103), 357-373.
- Reeh, N. (1988), A flow-line model for calculating the surface profile and the velocity, strain-rate, and stress fields in an ice sheet, J. Glaciol., 34(116), 46-54.
- Rignot, E. (2002), Ice-shelf changes in Pine Island Bay, Antarctica, J. Glaciol., 48(161), 247–256.

- Shepherd, A., D. J. Wingham, J. A. D. Mansley, and H. F. J. Corr (2001), Inland thinning of Pine Island Glacier, West Antarctica, *Science*, 291, 862–864.
- Shepherd, A., D. J. Wingham, and J. A. D. Mansley (2002), Inland thinning of the Amundsen Sea sector, West Antarctica, *Geophys. Res. Lett.*, 29(10), 1364, doi:10.1029/2001GL014183.
- Siegert, M. J., and A. J. Payne (2004), Past rates of accumulation in central West Antarctica, *Geophys. Res. Lett.*, 31, L12403, doi:10.1029/2004GL020290.
- Spikes, V. B., G. S. Hamilton, S. A. Arcone, S. Kaspari, and P. A. Mayewski (2004), Variability in accumulation rates from GPR profiling on the West Antarctic plateau, *Ann. Glaciol.*, *39*, 238–244.
- Steig, E. J., J. L. Fastook, C. Zweck, I. D. Goodwin, K. J. Licht, J. W. C. White, and R. P. Ackert (2001), West Antarctic ice sheet elevation changes, in *The West Antarctic ice sheet: Behavior and environment*, Ant. Res. Ser., vol 77, edited by R. B. Alley and R. A. Bindschadler, pp. 75–90, AGU, Washington, DC.
- Thompson, D. W. J., and J. M. Wallace (2000), Annular modes in the Extratropical Circulation. Part 1: Month-to-month variability, *J. Clim.*, 13, 1000–1016.
- van den Broeke, M. R., and N. P. M. van Lipzig (2004), Changes in Antarctic temperature, wind and precipitation in response to the Antarctic oscillation, *Ann. Glaciol.*, *39*, 119–126.
- van den Broeke, M., W. J. van de Berg, and E. van Meijgaard (2006), Snowfall in coastal West Antarctica much greater than previously assumed, *Geophys. Res. Lett.*, 33, L02505, doi:10.1029/2005GL025239.
- Waddington, E. D., J. F. Bolzan, and R. B. Alley (2001), Potential for stratigraphic folding near ice-sheet centers, *J. Glaciol.*, 47(159), 639–648.
- Waddington, E. D., H. Conway, E. J. Steig, R. B. Alley, E. J. Brook, K. C. Taylor, and J. W. C. White (2005), Decoding the dipstick: Thickness of Siple Dome, West Antarctica, at the last glacial maximum, *Geology*, 33(4), 281–284.
- G. A. Catania, H. Conway, S. F. Price, and E. D. Waddington, Department of Earth and Space Sciences, University of Washington, Seattle, WA 98195, USA.
- D. L. Morse, Institute for Geophysics, Jackson School of Geosciences, University of Texas at Austin, Austin, TX 78758, USA.
- T. A. Neumann, Department of Geology, University of Vermont, Burlington, 180 Colchester Ave., VT 05405, USA. (thomas.neumann@uvm.edu)